THE JOURNAL OF PHYSICAL CHEMISTRY B

 VOLUME 106, NUMBER 42, OCTOBER 24, 2002

LETTERS

Silver Nanodisks: Synthesis, Characterization, and Self-Assembly

Sihai Chen,* Zhiyong Fan, and David L. Carroll

Laboratory for Nanotechnology, School of Materials Science and Engineering, Clemson University, Clemson, South Carolina 29634

Received: June 24, 2002; In Final Form: August 28, 2002

A new form of silver nanostructured materials, silver nanodisks, are generated by a solution-phase approach. In this method, truncated triangular silver nanoplates are at first fabricated through seed-mediated growth of silver particles in the presence of concentrated cetyltrimethylammonium bromide (CTAB). Subsequent aging of the obtained triangular silver nanoplate solution at 40 °C leads to the formation of silver nanodisks. Transmission electron microscopy and atomic force microscopy studies show that the nanodisks have a thickness of the order of 20−30 nm and a diameter around 60 nm. X-ray and electron diffraction analyses reveal that the nanodisks are single crystals and with their basal plane as the (111) lattice plane. These nanodisks display a strong surface plasmon absorption band at 475 nm. The formation of a self-assembled monolayer of CTAB on the basal plane is suggested to account for both the anisotropic growth from triangular nanoplates to nanodisks and the formation of large-scale necklace-like nanostructures.

The shape of metal or semiconductor nanoparticles has received intensive attention in recent years due to its strong effect on the physical and chemical, including optical, electronic, magnetic and catalytic, properties of the nanomaterials.[1] For silver, preparation of different shaped nanoparticles has attracted special interest in optics,[2] surface enhanced Raman spectroscopy (SERS),[3] and biological labeling and diagnosis applications[4] because shape has been found to be a very sensitive factor in controlling the surface plasmon oscillation of particles. For example, based on the study of the plasmon resonance optical spectrum of individual nanoparticles, Schultz et al.[2] have shown that triangular particles can display peak plasmon resonance wavelengths mainly in the range of 600−700 nm while pentagons display in the range of 500−560 nm. Mirkin et al.[5] have also succeeded in the preparation of triangular nanoprisms, which displayed a strong in-plane dipole plasmon resonance at 670 nm. Note that these properties cannot be obtained using spherical particles through changing the sizes.[6]

Many differently shaped silver nanostructures have been observed or synthesized using various chemical approaches. Size controlled spherical particles have been obtained in micelle solution[7] or through seed-mediated growth processes.[6] Tetrahedral particles have been prepared using an aerosol technique.[8] Recently the formation of silver nanocubes has also been reported.[9] Other observed particles have shapes such as triangular,[2,5,10] pentagonal,[2] hexagonal,[11] decahedral,[12] icosahedral, and cuboctahedral.[13] Further, a wide range of studies have addressed the production of silver nanorods and wires due to their potential applications in optics and as interconnects in nanoelectronics. These materials have been prepared by controlling growth kinetics in liquid solution,[14] using the inorganic templates such as carbon nanotubes,[15] mesoporous materials,[16] steps on the solid surface,[17] or organic templates such as calix[4]hydroquinone superstructures,[18] polymer materials,[19] DNA chains,[20] or micelles.[21] Also, dentritic nanostructures of silver have been generated.[14d,22] Here, we report the synthesis and characterization of a new kind of silver nanostructure, i.e., silver nanodisks, which are generated in large quantities using a

* Corresponding author. Fax: 864-656-5973. E-mail: chens@clemson.edu

10.1021/jp026376b CCC: $22.00
Published on Web 09/21/2002

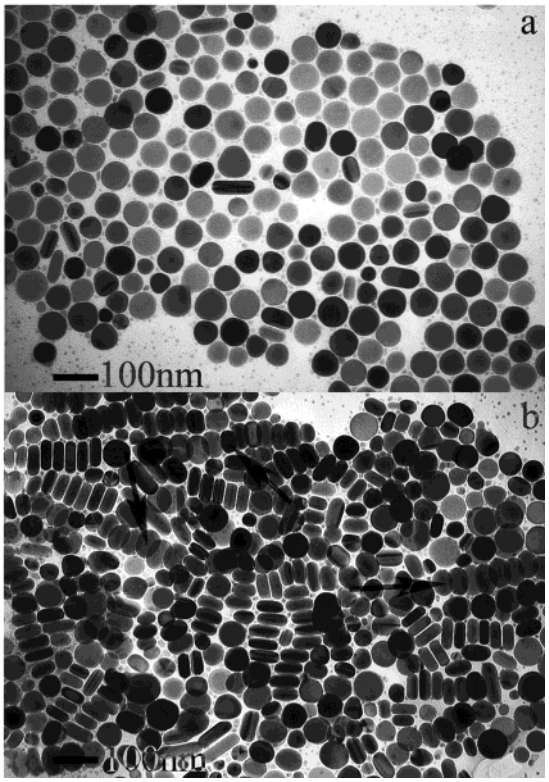

Figure 1. TEM images of the silver nanodisks obtained after 4 h aging at 40 °C. The particles in (a) lie flat on the substrates, while those in (b) stack together. The arrows in (b) show the partially stacked particles, giving ellipsoidal shape in projection.

solution-phase chemical approach. We found that the nanodisks display a strong surface plasmon band at around 475 nm. Furthermore, we can tune this band within 420 nm to 560 nm through a mild aging process. In addition, since the top surface of these nanodisks is covered with a self-assembled monolayer of long-chain organic molecules, they provide an ideal model system that mimics the self-assembled monolayer on the surface. Due to their nanoscale sizes, silver nanodisks are expected to be applicable as building blocks in modern nanoelectronics.

Our synthetic procedure includes mainly two steps. The first step is the generation of the truncated triangular silver nanoplates, which are obtained by seed-mediated[23] growth of silver particles in the presence of concentrated cetyltrimethylammonium bromide (CTAB).[24] The second step is the aging of the triangular silver nanoplate solution at 40 °C for 4 h. Figure 1a shows the TEM image of the obtained silver nanodisks lying flat on the substrate. For most of the particles, outlines of round circles can be clearly defined. Measurement of the size distribution gives that the mean diameter and standard deviation of the particles are 59 ± 10 nm. To confirm the plate-like nature of these particles, tilt experiments were performed. It was found that the shape of the projection of these particles changes to ellipsoidal when the tilting angle changed from +60° to −60°; this clearly indicates that the particles are plates rather than spheres. The ellipsoidal shape observed due to the tilt of nanodisks can also be observed in some areas when they are partially stacked together (arrows in Figure 1b). Further evidence showing the plate-like nature of these particles is obtained when they closely self-assembled into chain-like structures (Figure 1b), making it easy to estimate their thickness (26 ± 3.4 nm). Observed from the side view, these nanoplates are round in edges and also look like rods; the aspect ratios of these images are between 2 and 3, which are consistent with the value of 2.3

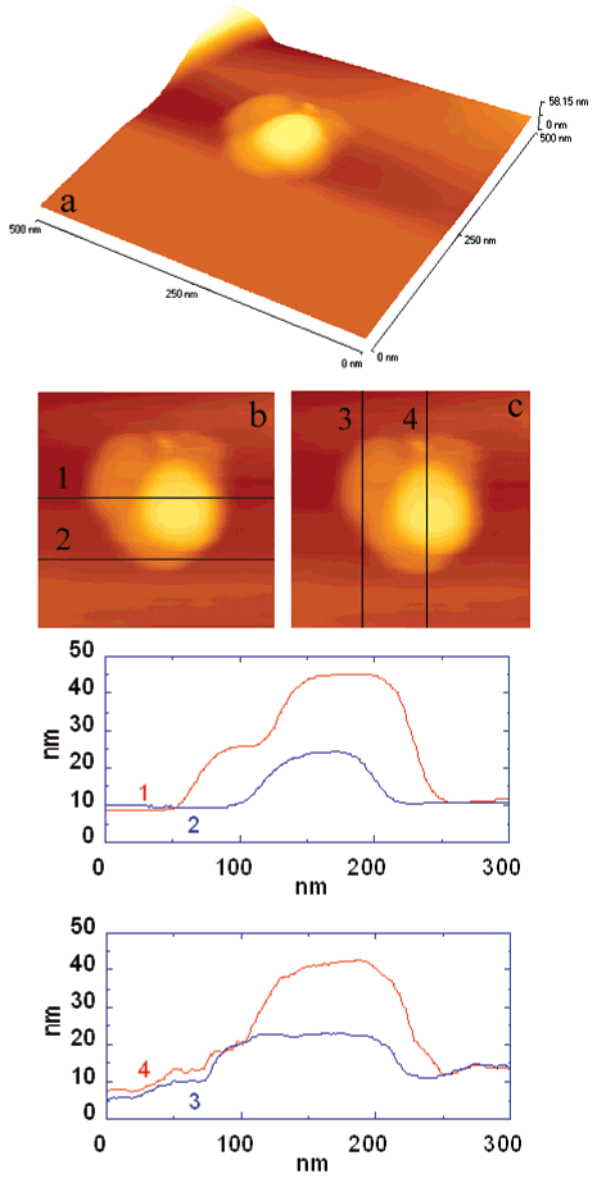

Figure 2. (a) Three-dimensional AFM images of several silver nanodisks stacked together. (b) Horizontal and (c) vertical line analyses of the nanodisks.

obtained by dividing average disk diameter by their thickness. Note that there are still gaps between the packed neighboring nanodisks with an average distance of 3−3.6 nm. Because the average molecular length of the C_{16} chain is about 1.8−1.9 nm,[26] this gap distance is almost double the length of the CTAB long alkyl chain. It suggests that the basal plane of each nanodisk may be covered with a monolayer of CTAB molecules, most likely, with its CH_3-N^+ headgroup bound to the silver surface and its long alkyl hydrophobic chain toward outside. It is the strong hydrophobic interactions between long alkyl chains on neighboring plates that cause the stacking of the nanodisks. The similar double alkyl layer structures for CTAB have already been suggested on Au nanorod surfaces.[27]

AFM was further used to define the nanodisk shapes. Figure 2a gives the three-dimensional image of four stacked silver nanodisks. The line analysis (Figure 2 b and c) shows that these plates have thicknesses around 20 nm and diameters of 50−90 nm, which is consistent with the TEM observations shown above. It is important to notice the flatness of the top surface of these nanodisks (lines 1 to 4 in Figure 2).

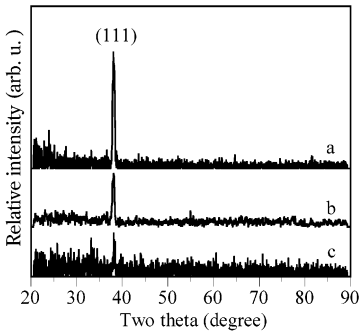

Figure 3. OPML-XRD patterns of the silver particles obtained before (a), after 5 min, (b) and 4 h (c) of aging at 40 °C.

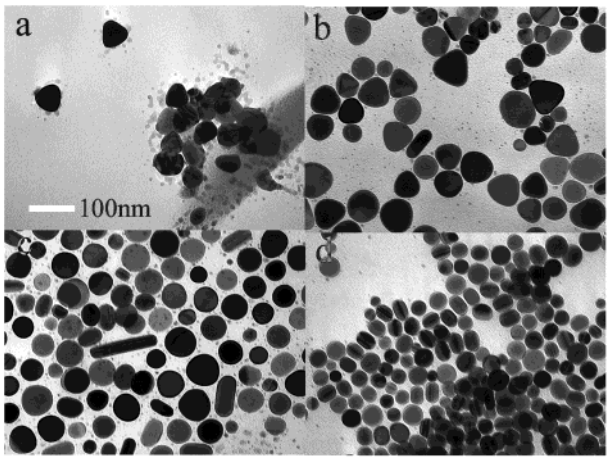

Figure 4. TEM images of the silver particles obtained (a) before and (b) after 5 min, (c) 4 h, and (d) 57 h of aging at 40 °C. The sample in (a) is prepared without centrifugation, through directly dropping the solution on the copper grid, followed by washing with copious amounts of deionized water and dried. The scale bar in (a) applies to all images.

Structure information is obtained with electron diffraction and oriented particulate monolayer X-ray diffraction (OPML-XRD) analyses. Electron diffraction of individual silver nanodisks gives spot points with a hexagonal arrangement, indicating that the particle is a single crystal. The XRD patterns (Figure 3c) for the flat-lying nanodisks with their basal plane parallel to the substrate show only an overwhelmingly intensive diffraction peak at $2\Theta = 38.05$, which is from the (111) lattice plane of face-centered cubic (fcc) silver. This clearly demonstrates that the particles are made of pure silver and their basal plane, i.e., the top crystal plane, should be the (111) plane. For the plate-like metal particles, this structural configuration has been found to be quite common, for example, similar cases have also been reported for silver,[5] nickel,[28] copper,[29] and gold[30] plates. It is highly possible that this plane may possess the lowest surface tension, as in the studies shown for the {111} plane of lead crystals.[31] Also, the adsorption of CTAB monolayer on this plane should play an important role in lowering the surface tension and stabilizing the plates.

In our synthetic procedure, the aging process has been found to exert a strong influence on the shape of the silver particles. To clearly elucidate this process, samples obtained at different aging times at 40 °C are studied. Figure 4a shows the TEM image of the particles obtained before aging. One can see that most of the particles have triangular outlines. Interestingly, some small particles with sizes below 10 nm are also observed surrounding the particles; we thus suppose that these smaller particles may play an important role in the growth of large

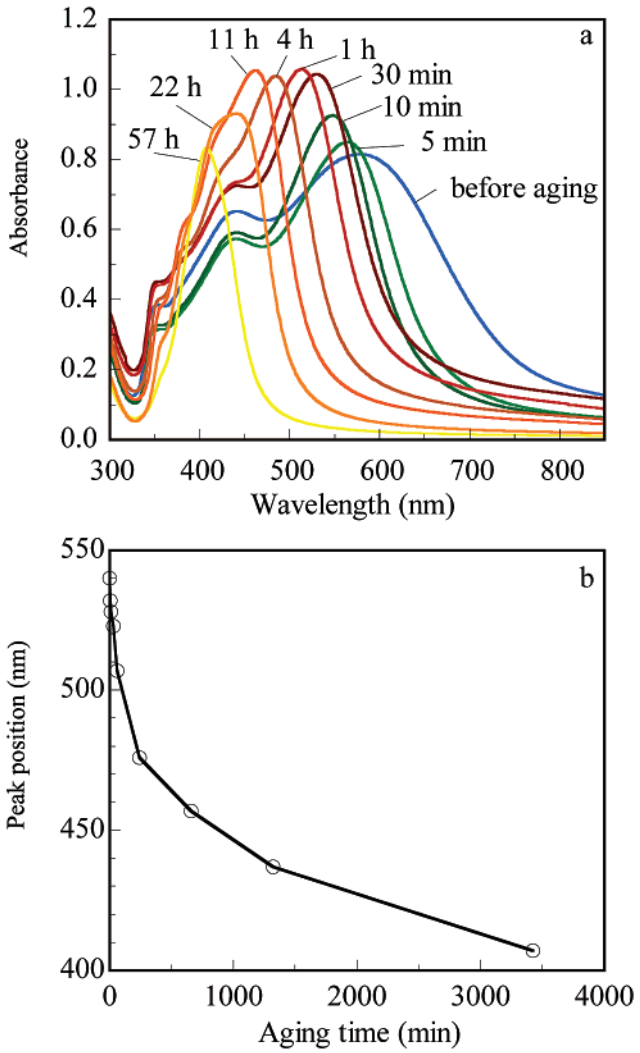

Figure 5. (a) Absorption spectra of the samples aged at 40 °C for different times. (b) Shift of the main absorption peak position with the aging time.

triangular particles through an "Ostwald ripening" process.[32] The presence of these small particles also supports the observation of a "seed-mediated nucleation process" reported by Jana et al.[33] because the size of our seeds are around 15 nm, which is larger than the observed small particles. As the aging time increased from 5 min to 4 h (Figure 4b and c), the particle shape changed from a truncated triangle to a circle. On the other hand, the particle thickness is essentially unchanged (24 ± 8 nm at 5 min vs 26 ± 3.4 nm at 4 h); similar OPML-XRD patterns are observed for the unaged, 5 min aged, and 4 h aged samples (Figure 3), implying that the (111) basal plane is not altered during this aging process. This shows that the anisotropic growth of silver mainly occurred at the edge {100} planes of the triangles. It is reasonable to suggest that CTAB molecules play a critical role in this anisotropic growth. A well-defined SAM layer of CTAB on the (111) plane should prevent this plane from further growth, leading to the rounding of the triangular particles.

Interestingly, after aging for a long time (e.g., 57 h), as shown in Figure 4d, the particles shrank in size to 44 ± 8 nm and changed to spherical in shape. Because this size is larger than the thickness but smaller than the diameter of nanodisks, particle growth normal to the basal plane should occur due to the desorption or destruction of the CTAB self-assembled monolayers. Similar aging effects are also reported for the gold

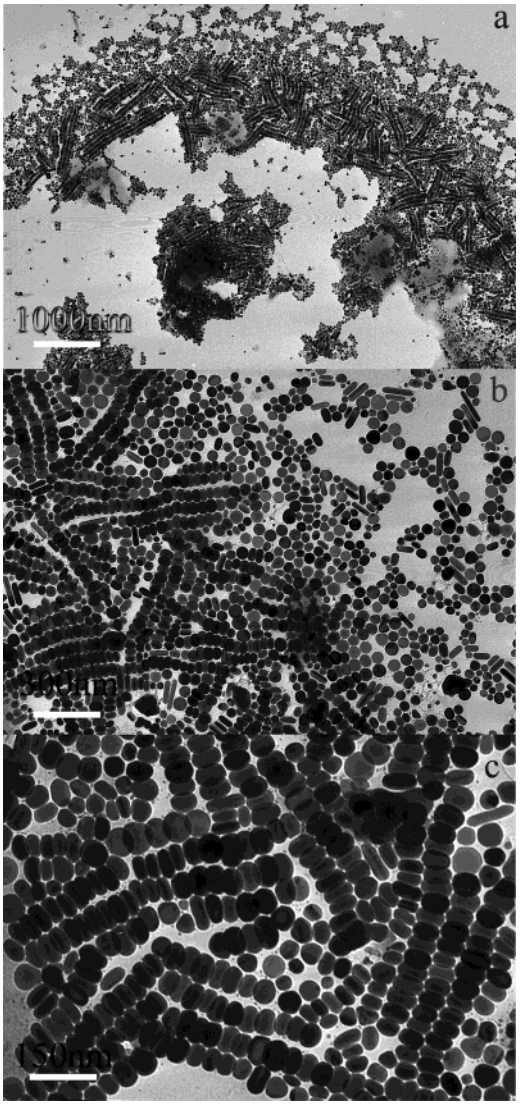

Figure 6. TEM images showing the formation of necklace-like structures due to the nanodisks partially stacked together. Images (a), (b), and (c) are obtained at different magnifications.

nanorods.[34] On the other hand, particle dissolution should also occur along the basal plane. This phenomenon is more apparent when aging is carried out at a higher temperature, such as 80 or 95 °C. In some cases, particles are completely dissolved, giving a colorless transparent solution. We suggest that high concentration of Br^- ions may play a role in assisting this dissolution process; further study is still under way.

The above shape changes are reflected in the absorption spectra (Figure 5a). Before aging, the spectrum of truncated triangular particles displays mainly three absorption peaks at 584, 444, and 351 nm. According to the theoretical calculation of Schatz et al.,[5] these peaks are assigned to in-plane dipole, out-of-plane dipole, and quadrupole plasmon resonances, respectively. When the aging time changed from 5 min to 4 h, the 584 nm peak quickly blue-shifted (see Figure 5b), corresponding to the in-plane shape transformation from triangle to circle. At the same time, the peak positions of the two out-of-plane peaks are kept almost unchanged due to the constant thickness of the nanoplates. Continuous aging to 57 h finally gave a single absorption band at 420 nm, which belongs to the spherical particles.

The nanodisks are found to form a large area of necklace-like structures on the copper grid (Figure 6). It is at present not clear whether these self-assembled structures are generated in solution or formed on the grid during solvent evaporation. However, at least two factors can be considered as prerequisites for generating these structures: one is the existence of the SAM layer on the basal plane of the nanodisks, which provides the hydrophobic interactions between neighboring particles; another is the monodispersity of the nanodisks. One can see that nanodisks in the trains are similar in size, whereas the rods or some smaller particles cannot form such structures (Figure 6 b, right part). These self-assembled structures provide an interesting example showing that nanodisks can be used as very useful building blocks in constructing devices in future nanoelectronics.

In summary, for the first time, silver nanodisks have been generated in large quantities by a solution-phase approach. These particles have thicknesses of 26 nm and diameters around 60 nm. They are single crystal and with their basal plane as (111) lattice plane. The formation of a self-assembled monolayer of CTAB on the basal plane is likely to be very important not only in explaining the anisotropic growth from triangular nanoplates to nanodisks but also in the formation of large-area necklace-like structures. A strong surface plasmon absorption band at 475 nm is found for these nanodisks. In addition, a simple mild aging method is provided to systematically control the surface plasmon band of silver particles within 420 nm to 560 nm.

Acknowledgment. We thank DARPA for support through grant N66001-01-1-8938 (the Laboratory for Advanced Photonic Composites).

Note Added after ASAP Posting. This article was released ASAP on 9/21/2002 with an error in ref 23. The correct version was posted on 9/26/2002.

References and Notes

(1) Creighton, J. A.; Eadon, D. G. *J. Chem. Soc., Faraday Trans.* **1991**, *87*, 3881. (b) Alivisatos, A. P. *Science* **1996**, *271*, 933. (c) Shi, J.; Babcock, G. K.; Awachalon, A. A. *Science* **1996**, *271*, 937. (d) Link, S.; El-Sayed, M. A. *J. Phys. Chem. B* **1999**, *103*, 8410. (e) Hu, J. T.; Odom, T. W.; Lieber, C. M. *Acc. Chem. Res.* **1999**, *32*, 435. (f) Wang, Z. L. *J. Phys. Chem. B* **2000**, *104*, 1153. (g) Hoelderich, W. F. *Catal. Today* **2000**, *62*, 115.

(2) Mock, J. J.; Barbic, M.; Smith, D. R.; Schultz, D. A.; Schultz, S. *J. Chem. Phys.* **2002**, *116*, 6755.

(3) Nie, S.; Emory, S. R. *Science* **1997**, *275*, 1102. (b) Kneipp, K.; Wang, Y.; Kneipp, H.; Perelman, L. T.; Itzkan, I.; Dasari, R. R.; Feld, M. S. *Phys. Rev. Lett.* **1997**, *78*, 1667.

(4) Schultz, S.; Smith, D. R.; Mock, J. J.; Schultz, D. A. *Proc. Natl. Acad. Sci. U.S.A.* **2000**, *97*, 996.

(5) Jin, R. C.; Cao, Y. W.; Mirkin, C. A.; Kelly, K. L.; Schatz, G. C.; Zheng, J. G. *Science* **2001**, *294*, 1901.

(6) Schneider, S.; Halbig, P.; Grau, H.; Nickel, U. *Photochem. Photobiol.* **1994**, *60*, 605.

(7) Taleb, A.; Petit, C.; Pileni, M. P. *Chem. Mater.* **1997**, *9*, 950. (b) Taleb, A.; Petit, C.; Pileni, M. P. *J. Phys. Chem. B* **1998**, *102*, 2214.

(8) Harfenist, S. A.; Wang, Z. L.; Alvarez, M. M.; Vezmar, I.; Whetten, R. L. *J. Phys. Chem.* **1996**, *100*, 13 904. (b) Harfenist, S. A.; Wang, Z. L.; Alvarez, M. M.; Vezmar, I.; Whetten, R. L. *Adv. Mater.* **1997**, *9*, 817. (c) Alvarez, M. M.; Vezmar, I.; Whetten, R. L. *J. Aerosol. Sci.* **1998**, *29*, 115. (d) Wang, Z. L.; Harfenist, S. A.; Vezmar, I.; Whetten, R. L.; Bentley, J.; Evans, N. D.; Alexander, K. N. *Adv. Mater.* **1998**, *10*, 808.

(9) Sun, Y.; Mayers, B. T.; Xia, Y. *Nano Lett.* **2002**, *2*, 481.

(10) Kirkland, A. I.; Jefferson, D. A.; Duff, D. G.; Edward, P. P.; Gameson, Johnson, B. F. G.; Smith, D. J. *Proc. R. Soc. London A* **1993**, *440*, 589.

(11) Klaus, T.; Joerger, R.; Olsson, E.; Granqvist, C.-G. *Proc. Natl. Acad. Sci. U.S.A.* **1999**, *96*, 13611.

(12) Duff, D. G.; Curtis, A. C.; Edwards, P. P.; Jefferson, D. A.; Johnson, B. F. G.; Logan, D. E. *J. Chem. Soc., Chem. Commun.* **1987**, 1264. (b) Giorgio, S.; Urban, J. *Appl. Phys. Lett.* **1988**, *52*, 1467.

(13) Giorgio, S.; Urban, J. *J. Phys. F: Met. Phys.* **1988**, *18*, L147.

(14) Zhou, Y.; Yu, S. H.; Wang, C. Y.; Li, X. G.; Zhu, Y. R.; Chen, Z. Y. *Adv. Mater.* **1999**, *11*, 850. (b) Zhou, Y.; Yu, S. H.; Cui, X. P.; Wang, C. Y.; Chen, Z. Y. *Chem. Mater.* **1999**, *11*, 545. (c) Zhu, J.; Liu, S.; Palchik, O.; Koltypin, Y.; Gedanken, A. *Langmuir* **2000**, *16*, 6396. (d) Zhang, D.; Qi, L.; Ma, J.; Cheng, H. *Chem. Mater.* **2001**, *13*, 2753. (e) Liu, S.; Yue, J.; Gedanken, A. *Adv. Mater.* **2001**, *13*, 656. (f) Sun, Y.; Gates, B.; Mayers, B.; Xia, Y. *Nano Lett.* **2002**, *2*, 165. (g) Sun, Y.; Xia, Y. *Adv. Mater.* **2002**, *14*, 833.

(15) Ajayan, P. M.; Iijima, S. *Nature* **1993**, *361*, 333. (b) Ugarte, D.; Chatelain, A.; de Heer, W. A. *Science* **1996**, *274*, 1897.

(16) Han, Y. J.; Kim, J. M.; Stucky, G. D. *Chem. Mater.* **2000**, *12*, 2068. (b) Huang, M. H.; Choudrey, A.; Yang, P. *Chem. Commun.* **2000**, 1063.

(17) Song, H. H.; Jones, K. M.; Baski, A. A. *J. Vac. Sci. Technol. A* **1999**, *17*, 1696. (b) Zach, M. P.; Ng, K. H.; Penner, R. M. *Science* **2000**, *290*, 2120.

(18) Hong, B. H.; Bae, S. C.; Lee, C.-W.; Jeong, S.; Kim, K. S. *Science* **2001**, *294*, 348.

(19) Nhattacharrya, S.; Saha, S. K.; Chakravorty, D. *Appl. Phys. Lett.* **2000**, *76*, 3896.

(20) Braun, E.; Eichen, Y.; Sivan, U.; Ben-Yoseph, G. *Nature* **1998**, *391*, 775.

(21) Jana, N. R.; Gearheart, L.; Murphy, C. J. *Chem. Commun.* **2001**, 617. (b) El-Sayed, M. A. *Acc. Chem. Res.* **2001**, *34*, 257. (c) Murphy, C. J.; Jana, N. R. *Adv. Mater.* **2002**, *14*, 80.

(22) Xiao, J.; Xie, Y.; Tang, R.; Chen, M.; Tian, X. *Adv. Mater.* **2001**, *13*, 1887.

(23) 0.6 mL of 10 mM $NaBH_4$ (Alfa Aesar, 98%) was rapidly injected into the stirring mixture containing 0.5 mL of 10 mM $AgNO_3$ (Alfa Aesar, 99.9%) and 20 mL of 1.25 mM sodium citrate (Alfa Aesar, 99%). The resultant solution was slowly stirred for 3 min and aged for 2 h before use. The particle sizes are found to be 15 ± 6 nm.

(24) A particle growth solution was prepared: 2.5 mL of 10 mM $AgNO_3$, 5 mL of 100 mM L-ascorbic acid (Alfa Aesar, 99%), 73 mL of 0.1 M CTAB (Alfa Aesar, 99%), and 2.5 mL of silver seeds. To this solution, 1 mL of 1 M NaOH (Alfa Aesar, 99.996%) was rapidly added. With gently shaking, the color of the solution changed from light yellow to brown, to red, and finally to green within 5 min. A similar recipe was used for the synthesis of silver nanowires (ref 21a), but we use a higher concentration of NaOH, which proved critical for triangular particle formation. A Hitachi H-7000 transmission electron microscope (TEM), operated at 100 kV, was used to observe the images. The specimens were prepared by dropping the solution (centrifuged at 3000*g* for 10 min to remove the surfactant, if not otherwise stated) on the copper grids covered with Formvar and amorphous carbon, and let dry in air. Atomic force microscopy (AFM) studies were conducted with a Topometrix TM 2010, operated in noncontact mode. The sample was prepared by dropping the solution on a silicon wafer and drying in air. UV−vis absorption spectra were obtained on a Perkin-Elmer Lambda 900 spectrophotometer. Oriented particulate monolayer X-ray diffraction (OPML-XRD)[25] was used to determine the Miller indices of the basal plane of the nanoplates, performed on a Scintag DXS 2000 diffractometer with the X-ray generator (Cu Kα radiation, $\lambda = 0.15418$ nm) operated at 40 kV and 30 mA. The samples were prepared by dispersing the nanoplates into 3% gelatin (at 40 °C) on a glass plate, spreading the solution evenly with a glass stick, and letting it dry naturally in air.

(25) Sugimoto, T.; Muramatsu, A.; Sakata, K.; Shindo, D. *J. Colloid Interface Sci.* **1993**, *158*, 420.

(26) Terrill, R. H.; Postlethwaite, T. A.; Chen, C.; Poon, C.; Terzis, A.; Chen, A.; Hutchison, J. E.; Clark, M. R.; Wignall, G.; Londono, J. D.; Superfine, R.; Falvo, M.; Johnson, C. S.; Samulski, E. T., Jr.; Murray, R. W. *J. Am. Chem. Soc.* **1995**, *117*, 12537.

(27) Mikoobakht, B.; El-Sayed, M. A. *Langmuir* **2001**, *17*, 6368.

(28) Bradley, J. S.; Tesche, B.; Busser, W.; Maase, M.; Reetz, M. T. *J. Am. Chem. Soc.* **2000**, *122*, 4631.

(29) Curtis, C.; Duff, D. G.; Edwards, P. P.; Jefferson, D. A.; Johnson, B. F. G.; Kirkland, A. I.; Wallace, A. S. *Angew. Chem., Int. Ed. Engl.* **1988**, *27*, 1530.

(30) Turkevich, J.; Stevenson, P. C.; Hillier, J. *J. Discuss. Faraday Soc.* **1951**, *11*, 55. (b) Bruche, B. *Kolloid-Z.* **1960**, *170*, 97. (c) Chiang, Y. S.; Turkevich, J. *J. Colloid Sci.* **1963**, *18*, 772. (d) Milligan, W. O.; Morriss, R. H. *J. Am. Chem. Soc.* **1964**, *86*, 3461. (e) Kirkland, A. I.; Edwards, P. P.; Jefferson, D. A.; Duff, D. G. *Annu. Rep. Prog. Chem. Sect. C* **1990**, *87*, 247. (f) Zhou, Y.; Wang, C. Y.; Zhu, Y. R.; Chen, Z. Y. *Chem. Mater.* **1999**, *11*, 2310.

(31) Heyraud, J. C.; Metois, J. J. *Surf. Sci.* **1983**, *128*, 334.

(32) Roosen, A. R.; Carter, W. C. *Physica A* **1998**, *261*, 232.

(33) Jana, N. R.; Gearheart, L.; Murphy, C. J. *Chem. Mater.* **2001**, *13*, 2313.

(34) Mohamed, M. B.; Ismail, K. Z.; Link, S, El-Sayed, M. A. *J. Phys. Chem. B* **1998**, *102*, 9370.